ORGANIC LETTERS

2012
Vol. 14, No. 12
3162–3165

Fluorescence Switching of Imidazo[1,5-*a*]pyridinium Ions: pH-Sensors with Dual Emission Pathways

Johnathon T. Hutt, Junyong Jo, András Olasz, Chun-Hsing Chen, Dongwhan Lee,* and Zachary D. Aron*

Department of Chemistry, Indiana University, 800 East Kirkwood Avenue, Bloomington, Indiana 47405, United States

dongwhan@indiana.edu; zaron@indiana.edu

Received May 7, 2012

ABSTRACT

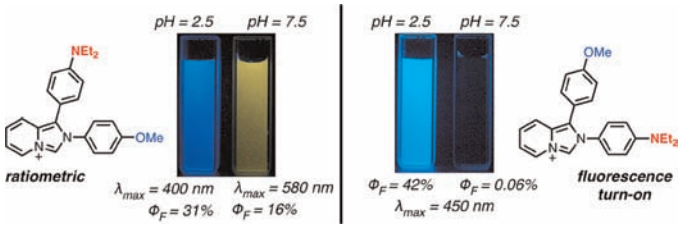

Imidazo[1,5-*a*]pyridinium ions are identified as highly emissive and water-soluble fluorophores accessed by an efficient three-component coupling reaction. Synthetic modifications of groups conjugated to the polyheterocyclic core are shown to profoundly impact the emission properties of these molecules. Notably, two structural isomers of functionalized imidazo[1,5-*a*]pyridinium ions were found to exhibit distinct de-excitation pathways, which are responsible for either a fluorescence turn-on or ratiometric response to pH change.

Small-molecule fluorophores are emerging as important tools for visualizing analytes of biological relevance.[1] Quantitative data can readily be obtained for specific targets by operationally simple detection schemes exploiting binding-induced perturbations of de-excitation pathways such as photoinduced electron transfer (PET) or intramolecular charge transfer (ICT). Changes in the intensity and/or wavelength of light emitted from molecular probes have been used in the detection of heavy metal ions[2] and anionic metabolites;[3] in the labeling of amino acids, peptides, nucleotides, and other macromolecules;[4] and for monitoring reactive oxygen/nitrogen species.[5] Although existing fluorogenic platforms including BODIPY, coumarin, naphthalimide, or fluorescein can be functionalized to display either ratiometric dual-emission (through ICT) or change in fluorescence intensity (through PET), structural modifications that control excited-state photophysics typically entail low-yielding multistep synthetic operations.[6] Fluorescent probes operating in biological systems must also exhibit water solubility, insensitivity to local polarity, and minimal interference from background emission, requirements which further highlight the ongoing challenges in this area.

In this paper, we disclose the structural and photophysical properties of water-soluble imidazo[1,5-*a*]pyridinium ion fluorophores that are readily prepared by a facile three-component coupling (Scheme 1).[7] In both organic and

(1) (a) de Silva, A. P.; Gunaratne, H. Q. N.; Gunnlaugsson, T.; Huxley, A. J. M.; McCoy, C. P.; Rademacher, J. T.; Rice, T. E. *Chem. Rev.* **1997**, *97*, 1515–1566. (b) Han, J.; Burgess, K. *Chem. Rev.* **2010**, *110*, 2709–2728. (c) Berezine, M. Y.; Achilefu, S. *Chem. Rev.* **2010**, *110*, 2641–2684. (d) Que, E. L.; Domaille, D. W.; Chang, C. J. *Chem. Rev.* **2008**, *108*, 1517–1549.

(2) (a) Chen, X.; Pradhan, T.; Wang, F.; Kim, J. S.; Yoon, J. *Chem. Rev.* **2012**, *112*, 1910–1956. (b) Quang, D. T.; Kim, J. S. *Chem. Rev.* **2010**, *110*, 6280–6301. (c) Nolan, E. M.; Lippard, S. J. *Chem. Rev.* **2008**, *108*, 3443–3480.

(3) (a) Duke, R. M.; Veale, E. B.; Pfeffer, F. M.; Kruger, P. E.; Gunnlaugsson, T. *Chem. Soc. Rev.* **2010**, *39*, 3936–3953. (b) Zhou, Y.; Xu, Z.; Yoon, J. *Chem. Soc. Rev.* **2011**, *40*, 2222–2235.

(4) (a) Kobayashi, H.; Ogawa, M.; Alford, R.; Choyke, P. L.; Urano, Y. *Chem. Rev.* **2010**, *110*, 2620–2640. (b) Gonçalves, M. S. T. *Chem. Rev.* **2009**, *109*, 190–212. (c) Beija, M.; Afonso, C. A. M.; Martinho, J. M. G. *Chem. Soc. Rev.* **2009**, *38*, 2410–2433.

(5) Chen, X.; Tian, X.; Shin, I.; Yoon, J. *Chem. Soc. Rev.* **2011**, *40*, 4783–4804.

(6) (a) Loudet, A.; Burgess, K. *Chem. Rev.* **2007**, *107*, 4891–4932. (b) Urano, Y.; Kamiya, M.; Kanda, K.; Ueno, T.; Hirose, K.; Nagano, T. *J. Am. Chem. Soc.* **2005**, *127*, 4888–4894. (c) Miura, T.; Urano, Y.; Tanaka, K.; Nagano, T.; Ohkubo, K.; Fukuzumi, S. *J. Am. Chem. Soc.* **2003**, *125*, 8666–8671. (d) Wang, H.; Wu, H.; Xue, L.; Shi, Y.; Li, X. *Org. Biomol. Chem.* **2011**, *9*, 5436–5444.

(7) Hutt, J. T.; Aron, Z. D. *Org. Lett.* **2011**, *13*, 5256–5259.

10.1021/ol3012524
Published on Web 06/06/2012

aqueous environments, these molecules exhibit high quantum-yield emissions whose wavelength can be systematically modified through varying substituents on the polyheterocyclic core. Notably, installation of a proton-binding amino group to the extended π-system furnished pH-responsive fluorophores, the de-excitation pathways of which could be switched between PET and ICT by *conformational control*.

Scheme 1. Synthesis and Emissive Properties of Functionalized Imidazo[1,5-*a*]pyridinium Ions[a]

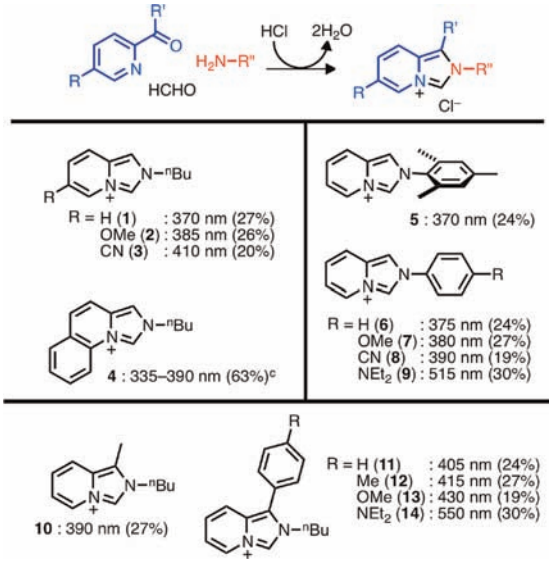

[a] For each compound, the maximum emission wavelength ($\lambda_{max,em}$) in MeCN is provided along with the fluorescence quantum yield (Φ_F) in parentheses. [b] Select compounds (see Supporting Information) were purified by anion metathesis to replace Cl^- with PF_6^- or BPh_4^-; variation of anions resulted in negligible changes in emission properties (see Supporting Information, Figures S1–S6). [c] Broad emission with multiple vibronic features.

In our investigations of imidazo[1,5-*a*]pyridinium ions as synthetic precursors to *N*-heterocyclic carbene (NHC) ligands,[7] we observed that these polyheterocyclic cations were highly fluorescent. As shown in Scheme 1, the simple derivative **1** has a high emission quantum yield of Φ_F = 27% in MeCN. Although the efficient radiative decay of selected imidazo[1,5-*a*]pyridinium ions and related structures have previously been reported,[8] the general structure–property relationships and potential utility of these fluorophores have remained largely unexplored. Additionally, studies of neutral imidazo[1,5-*a*]pyridines have shown that substitution at the C3 position of the imidazole ring modulates the emission properties of the molecule.[9]

Accordingly, we decided to systematically study how the substitution (**1**–**3**) and expansion (**4**) of the pyridine ring component of the molecule would influence its optical properties. As shown in Scheme 1 and Table S1, both **2** and **3** exhibit red-shifted absorption/emission relative to the benchmark system **1** (Figure S6). Annulation of the imidazo[1,5-*a*]pyridinium ion ring system to afford **4** resulted in a significant enhancement in Φ_F to 63%.

The effect of altering the *N*-substituent on the imidazole component of the molecule was studied using compounds **5**–**9** (Scheme 1; Table S2). Consistent with the trend observed for compounds **1**→**2**→**3**, a systematic red shift in the emission spectrum was observed along the series of **6**→**7**→**8** (overall $\Delta\lambda_{em}$ = 20 nm, Table S2). The UV–vis and fluorescence spectra of **1** and **5** are essentially superimposable, presumably resulting from deconjugation of the *N*-aryl unit from the imidazo[1,5-*a*]pyridinium ion core caused by steric congestion introduced by two *ortho*-substituents (Figure S7).

In contrast to the gradual spectral shift observed with methoxy and cyano substituents, a dramatic red shift ($\Delta\lambda_{em}$ = 140 nm) was observed upon incorporating an amino substituent (**6**→**9**, Figure S7). FMO analysis based on a density functional theory (DFT) energy-minimized model of **9** (Figure 1) revealed that its HOMO is dominated by the electron-donating *N*-aryl unit whereas its LUMO resides predominantly on the ring-fused cationic core. The calculated electronic structure is thus consistent with an ICT-type transition to access excited-states having a significant charge-separated character, the de-excitation from which gives rise to the observed longer-wavelength emission.[13] In support of this hypothesis, protonation of **9** resulted in a large ($\Delta\lambda_{em}$ = 140 nm) blue shift in its emission (Figure S9a).[14] With the disengagement of nitrogen lone-pair electrons from the extended π-conjugation, access to the ICT state is effectively suppressed. Consequently, protonated **9** (λ_{em} = 375 nm) "behaves" like simple aryl-substituted analogue **6**.

In order to introduce structural variations at the C1 position of the imidazo[1,5-*a*]pyridinium ion core, compounds **10**–**14** were prepared (Scheme 1). Installation of aryl groups (**11**–**14**) in place of a simple methyl group (**10**) at C1 resulted in a significant improvement in both emission quantum yields and spectral red shifts (Table S3; Figure S10). Notably, incorporation of a *p*-(*N*,*N*-diethylamino)phenyl substituent in compound **14** resulted in an intense emission at λ_{em} = 550 nm. Its large ($\Delta\lambda_{em}$ = 145 nm) bathochromic shift relative to the

(8) (a) Campbell, E. C.; Glover, E. E.; Trenholm, G. *J. Chem. Soc. C* **1969**, *15*, 1987–1990. (b) Mukherjee, A.; Dhar, S.; Nethaji, M.; Chakravarty, A. R. *Dalton Trans.* **2005**, 349–353. (c) Boydston, A. J.; Pecinovsky, C. S.; Chao, S. T.; Bielawski, C. W. *J. Am. Chem. Soc.* **2007**, *129*, 14550–14551. (d) Boydston, A. J.; Vu, P. D.; Dykhno, O. L.; Chang, V.; Wyatt, A. R.; Stockett, A. S.; Ritschdorff, E. T.; Shear, J. B.; Bielawski, C. W. *J. Am. Chem. Soc.* **2008**, *130*, 3143–3156. (e) Roy, M.; Chakravarthi, B. V. S. K.; Jayabaskaran, C.; Anajali, A. K.; Chakravarty, A. R. *Dalton Trans.* **2011**, *40*, 4855–4864.

(9) (a) Shibahara, F.; Sugiura, R.; Yamaguchi, E.; Kitagawa, A.; Murai, T. *J. Org. Chem.* **2009**, *74*, 3566–3568. (b) Yamaguchi, E.; Shibahara, F.; Murai, T. *J. Org. Chem.* **2011**, *76*, 6146–6158.

(10) Bissell, R. A.; de Silva, A. P.; Gunaratne, H. Q. N.; Lynch, P. L. M.; Maguire, G. E. M.; Sandanayake, K. R. A. S. *Chem. Soc. Rev.* **1992**, *21*, 187–195.

(11) (a) Maus, M.; Rettig, W.; Jonusauskas, G.; Lapouyade, R.; Rullière, C. *J. Phys. Chem. A* **1998**, *102*, 7393–7405. (b) Maus, M.; Rettig, W.; Bonafoux, D.; Lapouyade, R. *J. Phys. Chem. A* **1999**, *103*, 3388–3401. (c) Maus, M.; Rurack, K. *New J. Chem.* **2000**, *24*, 677–686. (d) Rurack, K.; Resch-Genger, U. *Chem. Soc. Rev.* **2002**, *31*, 116–127.

(12) Pankratov, A. N.; Uchaeva, I. M.; Doronin, S. Y.; Chernova, R. K. *J. Struct. Chem* **2001**, *42*, 739–746.

(13) In contrast, **6** lacking such an electron-donor group has both its HOMO and LUMO localized at the imidazopyridinium core (Figure S8).

(14) Under similar conditions, **1** shows no significant change in emission (see Figure S11 in the Supporting Information).

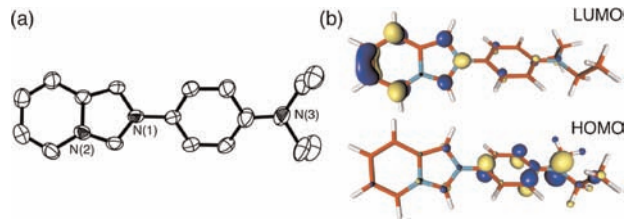

Figure 1. (a) ORTEP diagram of **9** with thermal ellipsoids at 50% probability. The diethylamino groups are disordered over two positions, for which only one model is shown. (b) FMO isosurface plots (cutoff = 0.05) of the DFT model of **9**.

reference system **11** is reminiscent of the behavior of **9** (vide infra) and implicates the involvement of charge-separated excited states. This postulation was confirmed by a protonation-induced blue shift of **14** (Figure S9b), which parallels the chemistry of **9**.

The intense ICT-type long-wavelength emissions observed for **9** and **14**, and the ability to modulate their optical properties, inspired us to prepare compounds **15** and **16** as structural analogues containing extended π-conjugation (Figure 2). It should be noted that initial attempts to access desmethoxy **15** were impaired by the competing copolymerization of aniline and formaldehyde,[15] whereas incorporation of the *para* substituent onto the aniline precursor suppressed this side reaction. As a regioisomeric pair of molecules, **15** and **16** differ only in the relative positioning of the two aryl groups that are attached to the common imidazo[1,5-*a*]pyridinium ion core. This seemingly minor structural variation, however, resulted in profoundly different luminescent properties as detailed below.

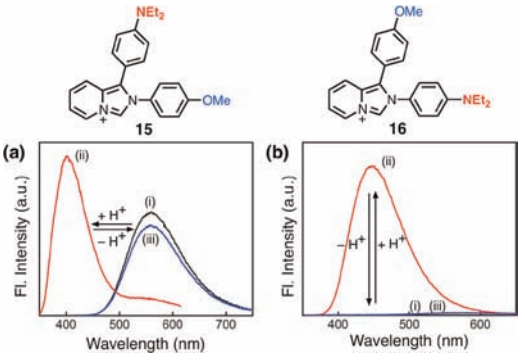

Figure 2. Emission spectra of (a) **15** and (b) **16** (= 30 μM) (as Cl^- salt) in MeCN, (i) prior to and (ii) after addition of CF_3CO_2H (60 mM), and (iii) after addition of DBU (90 mM) to the sample (ii). T = 298 K.

In MeCN, **15** showed an intense (Φ_F = 59%) yellow fluorescence at λ_{em} = 565 nm, which is further red-shifted than its simpler analogue **14** (Scheme 1). Upon acidification, the intensity of this band was diminished, with a new emission band emerging at λ_{em} = 400 nm (Figure 2a). Subsequent addition of DBU resulted in the disappearance of the emission at λ_{em} = 400 nm and reappearance of the emission at λ_{em} = 565 nm, demonstrating the reversibility of this process. In contrast to this ICT behavior seen with **15**, its regioisomer **16** displayed a broad and negligible (Φ_F < 0.2%) emission (Figure 2b). Addition of TFA, however, resulted in the appearance of an intense (Φ_F = 57%) band at λ_{em} = 450 nm. Subsequent addition of DBU quenched this fluorescence, demonstrating the reversible nature of this protonation-driven fluorescence turn-on/off switching.

The strikingly different emission properties of the two imidazo[1,5-*a*]pyridinium ion isomers **15** and **16** suggest that the *p*-dialkylaminophenyl group plays distinctively different roles in each case. For **15**, the aniline unit acts in a manner analogous to the corresponding substituent in **9** or **14**, producing an ICT-type emission. Protonation suppresses charge separation in the excited state, so that only local emission (LE) at higher energy is observed. For **16**, the aniline substituent participates in a PET-type de-excitation to quench fluorescence.[10] Upon protonation, however, its lone-pair electrons are no longer available for internal ET in the excited state. As a consequence, the inherent imidazo[1,5-*a*]pyridinium ion emission is restored. A question that immediately arises is what structural factors dictate the choice between ICT and PET made by the regioisomeric **15** and **16**.

Unlike their simpler analogues **9** and **14**, the presence of two aryl substituents in **15** and **16** introduces severe steric constraints that should prevent coplanar arrangement of the entire π-system. To investigate the effects of such structural distortion on the molecular photophysics, we have prepared a model system **17** (Figure 3) as an *electronically equivalent* but *sterically distorted* analogue of **9**.

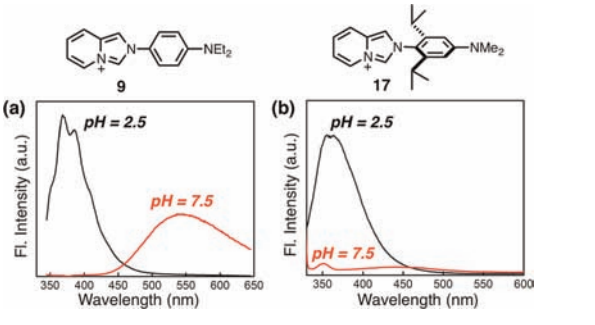

Figure 3. Emission spectra of (a) **9** (= 10 μM; as PF_6^- salt) and (b) **17** (= 5 μM; as BPh_4^- salt) in H_2O at pH = 7.5 (red) and pH = 2.5 (black). T = 298 K.

(15) Alger, M. *Polymer Science Dictionary*, 2nd ed.; Chapman & Hall: London, 1997; p 23.

(16) Compound **16** crystallizes in monoclinic space group $P2_1/c$ with a = 17.387(8) Å, b = 6.257(3) Å, c = 19.289(8) Å, β = 102.012(10)°, V = 2052.6(16) Å^3, and Z = 4. The structure of **16** was not fully refined due to poor crystal quality and low parameter to reflection ratio. Although detailed structural information cannot be provided, the chemical connectivity and twisting of the *N*-aryl group away from coplanarity with the imidazopyridinium ring portion of the molecule were unambiguously confirmed.

We anticipated that bulky isopropyl groups installed at *ortho*-positions should twist the aniline ring out of conjugation from the fluorogenic imidazo[1,5-*a*]pyridinium ion core of **17**. This effective deconjugation across the C−N bond indeed resulted in fluorescence quenching of **17** at pH = 7.5 (Figure 3b), whereas **9** remains emissive (λ_{em} = 550 nm; Figure 3a). At pH = 2.5, both molecules display strong fluorescence at λ_{em} = 360−375 nm. These findings are consistent with the ICT-type emission of **9** and PET-type relaxation of **17**, which can be controlled reversibly by straightforward acid−base chemistry. For twisted π-conjugated systems, a rapid intersystem crossing (ISC) and subsequent nonradiative relaxation could also make the molecule nonemissive.[11] This interpretation, however, cannot explain the recovery of fluorescence upon protonation that we observed.

An overlay of the X-ray structures of **16**[16] and **9** (Figure 4a) indeed shows that the presence of the *p*-methoxyphenyl substituent at C1 significantly increases the torsional angle between the *p*-diethylaminophenyl group and the imidazo[1,5-*a*]pyridinium ion ring system. Additionally, the crystallographically determined torsional angles of **16** correspond to a point in the potential energy surface (PES) contour plot that is only 1.1 kcal mol^{-1} above the DFT minimum energy structure (Figure 4b). As anticipated, a completely coplanar arrangement of the entire π-system ($\tau_1 = \tau_1 = 0°$) has to overcome severe steric congestion between two adjacent aryl groups, which would amount to a barrier ca. 22 kcal mol^{-1} higher in energy relative to the fully relaxed geometry. In contrast, adopting a near orthogonal orientation between the aniline ring and the imidazo[1,5-*a*]pyridinium ion core, i.e. $\tau_1 \rightarrow 90°$, is an energetically less costly process. This conformational preference of **16** might be responsible for the shift of de-excitation pathways from ICT to PET. Apparently, the ICT de-excitation pathway of **15** suffers less from this structural distortion, which results in strikingly different emission properties between the two regioisomers (Figure 2).

As positively charged imidazo[1,5-*a*]pyridinium ions, both **15** and **16** are readily water-soluble, which allowed us to investigate their pH-dependent emission properties in buffered aqueous solutions in detail. As shown in Figure 5, **15** displays a *ratiometric response to pH*, with nicely correlated increases and decreases in the emission intensity at $\lambda_{em,max}$ = 400 nm and $\lambda_{em,max}$ = 580 nm within the pH window of 2.5−7.5. In water at pH = 7.5, **16** remains essentially nonemissive (Φ_F = 0.06%), but lowering the pH resulted in a ca. 700-fold enhancement in cyan fluorescent intensity (Φ_F = 42% at pH = 2.5) at $\lambda_{em,max}$ = 450 nm to provide turn-on signaling. Nonlinear regression of the sigmoidal response of fluorescence intensity vs pH provided pK_a = 5.0 for **15** and pK_a = 4.4 for **16** (Figures S12 and S13). These values are significantly lower than that of *N,N*-diethylaniline (pK_a = 6.5)[12] and reflect the inductive effect of the cationic ring system.

In summary, we have demonstrated the potential utility of imidazo[1,5-*a*]pyridinium fluorophores. These compounds can be directly accessed through an efficient three-component coupling reaction, are highly fluorescent, and inherently water-soluble, making them ideal for customization for nearly any imaging need. Specifically, the relatively low pK_a value of these pH-sensitive fluorophores, operating either in a ratiometric fashion for precise determination of local pH values or in a turn-on/off fashion for visualization/imaging with high spatial resolution, is ideal for investigating acidic cellular environments with minimal interference from background fluorescence. Efforts are currently underway in our laboratories to develop target-oriented applications of these and related imidazo[1,5-*a*]pyridinium ion derivatives *in vivo*.

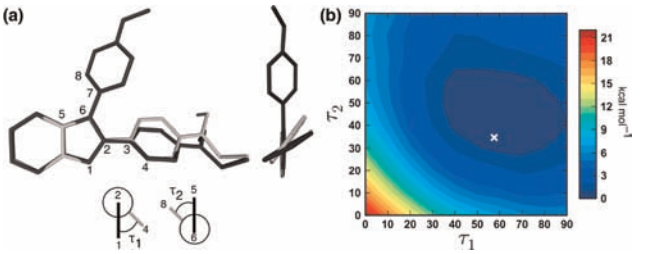

Figure 4. (a) An overlay of the X-ray structure of **9** (light gray) with that of **16** (black); selected atoms (1−8) are labeled to define the interplanar torsional angles τ_1 and τ_2. (b) PES contour plot of the DFT model of **16**, with a cross mark corresponding to the crystallographically determined structure of **16**.

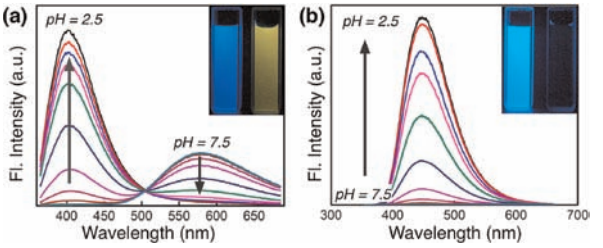

Figure 5. pH-Dependent changes in the emission spectra of (a) **15** and (b) **16** (30 μM) in water. Inset images: aqueous solution samples under UV-lamp at pH = 2.5 (left) and 7.5 (right).

Acknowledgment. D.L. thanks DTRA/Army Research Office (W911NF-07-1-0533), and Z.D.A. thanks Indiana University for financial support of this work.

Supporting Information Available. Experimental procedures for all compounds generated through this work, and spectroscopic, X-ray crystallographic, and computational data. This material is available free of charge via the Internet at http://pubs.acs.org.

The authors declare no competing financial interest.